



Article

Inhibitory Effects of Cu₂O/SiO₂ on the Growth of *Microcystis aeruginosa* and Its Mechanism

Gongduan Fan ^{1,*} , Minchen Bao ¹, Bo Wang ^{2,3,*}, Shimin Wu ², Lingxi Luo ², Binhui Li ² and JiuHong Lin ¹

¹ College of Civil Engineering, Fuzhou University, Fujian 350116, China; N170527002@fzu.edu.cn (M.B.); n190527070@fzu.edu.cn (J.L.)

² IER Environmental Protection Engineering Technology Co., Ltd., Shenzhen 518071, China; wushimin@gmail.com (S.W.); luolingxi1985@outlook.com (L.L.); libinhui2727@outlook.com (B.L.)

³ School of Urban Planning and Design, Shenzhen Graduate School, Peking University, Shenzhen 518055, China

* Correspondence: fgdfz@fzu.edu.cn (G.F.); 1801111800@pku.edu.cn (B.W.)

Received: 16 October 2019; Accepted: 17 November 2019; Published: 22 November 2019



Abstract: In this study, a novel nanomaterial Cu₂O/SiO₂ was synthesized based on nano-SiO₂, and the inhibitory effects of different concentrations of Cu₂O/SiO₂ on the growth of *Microcystis aeruginosa* (*M. aeruginosa*) were studied. At the same time, the mechanism of Cu₂O/SiO₂ inhibiting the growth of *M. aeruginosa* was discussed from the aspects of Cu²⁺ release, chlorophyll *a* destruction, oxidative damage, total protein, and the phycobiliprotein of algae cells. The results showed that low doses of Cu₂O/SiO₂ could promote the growth of *M. aeruginosa*. When the concentration of Cu₂O/SiO₂ reached 10 mg/L, it exhibited the best inhibitory effect on *M. aeruginosa*, and the relative inhibition rate reached 294% at 120 h. In terms of the algae inhibition mechanism, Cu₂O/SiO₂ will release Cu²⁺ in the solution and induce metal toxicity to algae cells. At the same time, *M. aeruginosa* might suffer oxidative damage by the free radicals, such as hydroxyl radicals released from Cu₂O/SiO₂, affecting the physiological characteristics of algae cells. Moreover, after the addition of Cu₂O/SiO₂, a decrease in the content of chlorophyll *a*, total soluble protein, and phycobiliprotein was found, which eventually led to the death of *M. aeruginosa*. Therefore, Cu₂O/SiO₂ can be used as an algacide inhibitor for controlling harmful cyanobacteria blooms.

Keywords: harmful cyanobacteria; Cu₂O/SiO₂; hydroxyl radical; antioxidant enzyme

1. Introduction

Excess nutrients (e.g., nitrogen and phosphorus) in the environment lead to the outbreak of harmful algal blooms (HABs) and the pollution of water sources [1], which caused wide concern [2]. HABs have a huge impact on human lives, production, and health. The cyanobacteria that spreads over the surface of the water will increase the turbidity of the lake and release some “unpleasant” taste to reduce the ornamental value of the water. The excessive reproduction and growth of cyanobacteria will consume dissolved oxygen, reduce the transparency of water, and change the pH, which has already threatened the human’s production and lives and the survival of aquatic animals and plants. What is worse, the death of cyanobacteria will release a variety of toxins (e.g., hepatotoxin and neurotoxin) that can cause serious long-term damage to human health [3].

Treatment schemes for controlling HABs have focused on the physical, chemical, and biological methods [4–6]. Most of those methods show promise, but hard to achieve safe and efficient applications in natural water bodies. In recent years, nanomaterials were widely used in algal growth inhibition, on account of the advantages of non-toxicity, high chemical stability, and strong adsorption capacity.

Wang et al. [7] observed that 100 mg/L TiO₂ will significantly inhibit the growth of *Chlamydomonas*. Zhao et al. [8] found that the growth inhibition rate of *Chlorella pyrenoidosa* exposed to 200 mg/L GO was more than 80%. Gu et al. [9] reported that the chlorophyll *a* removal rate of *M. aeruginosa* reached 80.6% in 2.5 h using 0.25 g/L Zn-Fe LDHs under visible light in photoreaction instrument equipped with a 300 W xenon lamp. Nevertheless, it must eliminate these defects, such as high cost, large dose, and the dependence on high-intensity irradiation to promote the nanomaterials applied as algicides in natural waters.

Cu-based nanomaterials can continuously inhibit the growth of cyanobacteria due to the characteristics that algae were sensitive to Cu²⁺ [10]. Cu₂O and modified-Cu₂O exhibit excellent photodegradability under low-intensity visible light [11,12], which makes it an ideal Cu-based nanomaterial for controlling HABs. Cu₂O is a common p-type semiconductor with a band gap of 2.0 to 2.2 eV. Cu₂O has attracted wide attention in the fields of catalysis, lithium batteries and sensors due to its good visible light response [13,14]. However, the e⁻/h⁺ pairs on Cu₂O cannot efficiently separate, which will lead to the fast recombination of the e⁻/h⁺ pairs, thus resulting in a decrease of the photocatalytic activity [15]. As a porous hydrophilic material, nano-SiO₂ has an -OH group on its surface and is often used as a matrix for nanomaterials [16]. The modification of Cu₂O with SiO₂ will increase the adsorption of organic substances on the surface acid sites and prevent the recombination of electron-hole pairs, which can improve the photocatalytic performance of Cu₂O/SiO₂. Besides, SiO₂ is commercially available and inexpensive, which makes the manufacturing cost of Cu₂O/SiO₂ greatly low.

Revealing the mechanism of growth inhibition of cyanobacterial cells by Cu₂O/SiO₂ will be helpful for its application in controlling HABs. Metal-containing nanomaterials will release metal ions into the solution, which can affect the growth of algae. Douglas et al. [17] found that the photosynthetic activity of *Dinoflagellates* decreased with increasing Cu²⁺ concentration. Franklin et al. [18] believed that Zn²⁺ released by ZnO will inhibit the growth of *Selenastrum bibraianum*. Sunandan et al. [19] found that Al³⁺ released by nano-Al₂O₃ reduced the cell viability of algae. Fan et al. [20] found that Cu²⁺ released by Cu-MOF-74 plays an important role on the growth inhibition of *M. aeruginosa*. Besides, nanomaterials could produce reactive oxygen species (ROSs) when in contact with the microorganisms. Common ROSs include H₂O₂, ·OH, and ·O₂⁻ [21,22]. When ROS were produced inside the cell, the antioxidant enzyme system, such as superoxide dismutase (SOD) and catalase (CAT), was activated to resist ROS and protect cells from oxidative damage. However, when the ROS content is too high for the cells to repair themselves, it will cause oxidative damage to the algae cells [23–25]. ·OH can react with terephthalic acid and then form 2,5-dihydroxyterephthalic acid, which can be excited by incident light and exhibit luminescence at 315 nm. The content of ·OH in the solution can be judged based on the fluorescence intensity [26,27]. Isopropyl alcohol (IPA) can inhibit the release of ·OH from nanomaterials, so it can be used as a quencher for ·OH [28]. Wang et al. [29] found that the DHA activity of *M. aeruginosa* was significantly inhibited from 654.06 U/L to 177.94 U/L after contacting F-Ce-TiO₂. Oukarroum et al. [30] found that the amount of ROS that was produced by *Chlorella* exposed to 10 mg/L nano-NiO for 96 h was 37 times higher than that of the control group. At the same time, the accumulation of ROS in algal cells led to lipid peroxidation, which caused the cell membrane to lose its integrity and selectively permeability [31]. The structure of the algae cells was destroyed, which caused a large amount of leakage of intracellular organic matter (IOM) and electrolytes, eventually leading to cell death.

The effect of nanomaterials on the photosynthetic system of algae cells includes two aspects: first, the effect on the light-harvesting ability of algae cells; second, the effect on chlorophyll. Algae are a kind of photoautotrophic organisms that undergo photosynthesis through photosynthetic pigments. Chlorophyll and phycobilin (PB) are the most important photosynthetic pigments in algae cells and they play an important role in photosynthesis. The PB is the main photosynthetic pigment in cyanobacteria and it usually combines with proteins to form phycobiliproteins (PBP). The PBPs of *M. aeruginosa* can be divided into phycocyanin (PC), phycoerythrin (PE), and allophycocyanin (APC) [32]. Gu et al. [33]

found that the removal rate of chlorophyll *a* by 0.4 g/L Cu₂O-montmorillonite was as high as 90.2%, when Cu₂O-montmorillonite was used to inhibit *M. aeruginosa*. Wang et al. [34] found that H₂O₂ inside the cells caused phycocyanin to detach from the thylakoid membrane.

In this study, a novel nanomaterial Cu₂O/SiO₂ was synthesized by the solution-phase method and characterized by X-ray diffraction (XRD), scanning electron microscope (SEM), and ultraviolet-visible spectroscopy (UV-Vis). Subsequently, the effects of Cu₂O/SiO₂ on photosynthetic pigments, total soluble protein, and phycobiliprotein of algae cells were studied. Finally, to reveal the mechanism of growth inhibition of *M. aeruginosa*, the interaction between Cu₂O/SiO₂ and algae cells were analyzed from the aspects of metal ion release, oxidative damage, and photosynthetic system damage. Overall, this study provides a theoretical basis for the application of Cu₂O/SiO₂ on control harmful cyanobacterial blooms.

2. Materials and Methods

2.1. Synthesis and Characterization of Cu₂O/SiO₂

Cu₂O/SiO₂ was prepared according to the following steps: 5 mL of CuCl₂(0.5 mol/L) and 1.9 g of nano-SiO₂ were first added to a mixture of 85 mL of deionized water and 20 mL of absolute ethanol. Afterwards, the mixture was transferred to a water bath at 40 °C. Later, 9 mL of NaOH (1 mol/L), 30 mL of absolute ethanol, and 9.8 mL of hydroxylamine hydrochloride were added and stirred well for 3 min. The mixture was centrifuged, washed, and dispersed in 50% ethanol and finally dried at 45 °C.

The synthesized Cu₂O/SiO₂ was characterized by scanning electron microscope (FEI, Helios G4 CX, Waltham, MA, USA), X-ray diffraction measurement (Rigaku, Ultima IV, Tokyo, Japan), and UV-Vis spectroscopy (PerkinElmer, LAMBDA 800 PE, Waltham, MA, USA).

2.2. Algae Growth Inhibition Experiment

2.2.1. Algae Cultures

Cyanobacterial species of *M. aeruginosa* (FACHB 905) were obtained from the Freshwater Algae Culture Collection of the Institute of Hydrobiology (FACHB) located in China. The strain was grown in BG-11 medium at 30 °C with illumination at 2000 Lux under 14L/10D cycle.

2.2.2. Cu₂O/SiO₂ Inhibit Algae Growth Experiment

The Cu₂O/SiO₂ stock solution (1000 mg/L) was obtained by adding 0.1 g of Cu₂O/SiO₂ into 100 mL deionized water. Subsequently, add 0, 0.01, 0.1, 0.5, 1, 2, and 5 mL of Cu₂O/SiO₂ stock solution to 100 mL of *M. aeruginosa* to achieve Cu₂O/SiO₂ concentrations of 0, 0.1, 1, 5, 10, 20, and 50 mg/L, respectively. Subsequently, algal cell density (OD₆₈₀) was determined by ultraviolet-visible spectrophotometer (Persee, New Century T6, Beijing, China) at 24-h intervals. The growth inhibition rate was calculated, as follows:

$$\mu_{i-j} = \frac{\ln X_j - \ln X_i}{t_j - t_i} \quad (1)$$

$$I_r = \frac{\mu_C - \mu_T}{\mu_C} \times 100\% \quad (2)$$

where, X_j is the OD₆₈₀ value of the sample at j (h); X_i is the OD₆₈₀ value of the sample at i (h); μ_{i-j} (%) is the specific growth rate of the sample; μ_C (%) is the average of the specific growth rates of the control group; μ_T (%) is the average of the specific growth rates of the experimental groups; and, I_r (%) is the inhibition rate that is based on the specific growth rate.

2.3. Mechanism Experiment of Cu₂O/SiO₂ Inhibiting Algae Growth

2.3.1. The Effect of Cu²⁺

Firstly, 1 mL of Cu₂O/SiO₂ stock solution (1000 mg/L) was added to 100 mL of deionized water to obtain a 10 mg/L Cu₂O/SiO₂ solution. Subsequently, the samples were filtered (0.22 μm membrane filter) and the Cu²⁺ concentration was then measured while using an inductively coupled plasma spectrometer (PerkinElmer, Optima 8000, USA) to determine the concentration of Cu²⁺ released from 10 mg/L Cu₂O/SiO₂. Finally, CuSO₄·5H₂O was selected as another source of Cu²⁺ to compare the effect of Cu²⁺ and Cu₂O/SiO₂ on the growth of *M. aeruginosa*. The concentration of CuSO₄·5H₂O in this experiment was the same as the concentration of Cu²⁺ released by 10 mg/L Cu₂O/SiO₂.

2.3.2. The Effect on Chlorophyll *a*

Cu₂O/SiO₂ stock solution was added to the *M. aeruginosa* and cultured under the same conditions in Section 2.2.2. The samples were taken every 24 h and the chlorophyll *a* content of the samples was spectrometrically determined according to the Chinese Environmental Protection Agency standard method [35]. The relative content of chlorophyll *a* was calculated by Equation (3).

$$\text{Relative content of chlorophyll } a \text{ (\%)} = (C/C_0) \times 100 \quad (3)$$

2.3.3. The Release of ·OH

Dissolve 2.0 mM terephthalic acid and excess NaOH in 400 mL of deionized water and stirred to fully dissolve. Subsequently, the pH of the solution was adjusted to approximately 7.0 with HCl. The above solution was evenly divided into two parts. Subsequently, Cu₂O/SiO₂ was added to the two groups of solutions, and 1 mM IPA was added to the control solution. After 2 h of the experiment, an aliquot of 5 mL of the sample was centrifuged at 3000× *g* for 5 min. Finally, the fluorescence intensity of the supernatant was measured with a fluorescence spectrometer (Edinburgh, FS5, Edinburgh, UK). Excitation (Ex): 250–450 nm in 5 nm steps, Emission (Em): 350–450 nm in 5 nm steps.

2.3.4. Active Species Trapping Experiments

For active species trapping experiments, isopropyl alcohol (IPA), benzoquinone (BQ), and sodium oxalate (SO), were utilized to trap ·OH, superoxide radicals ·O₂[−], and h⁺, respectively. The concentration of the scavengers was 0.01 mol/L. The whole process was designed similarly to Section 2.2.2.

2.3.5. The Effect on Antioxidant Enzyme

Firstly, 5 mL of the sample was centrifuged at 3000× *g* for 10 min. and the algal cell pellets were washed three times with PBS buffer solution. Then, the pellets were disrupted ultrasonically at 4 °C for 10 min. with 3 s pulses at 200 W by a cell sonicator (SCIENITZ JY92-II, Ningbo, China). Subsequently, in order to obtain the cell-free crude extract, algal cell debris was removed by centrifugation (3000× *g* for 10 min. at 4 °C). Finally, antioxidative enzymes (Superoxide dismutase, SOD; Catalase, CAT) were spectrophotometrically measured with commercial-available kits (Nanjing Jiancheng Bioengineering Institute, Nanjing, China).

2.3.6. Extracellular Organic Matter (EOM) & Intracellular Organic Matter (IOM)

The extracellular organic matter (EOM) and intracellular organic matter (IOM) of *M. aeruginosa* were extracted by the method of Tian and Qu et al. [36,37]. Fluorescence measurement of the EOM & IOM extract was conducted by using a fluorescence spectrometer; Ex was scanned from 200 to 450 nm, with a step of 5.0 nm, and Em from 200 to 550 nm with a step of 5.0 nm.

2.3.7. The Effect on Total Protein

The extraction method of the total protein (TP) from *M. aeruginosa* is referred to as the method of Tao et al. [38]. The coomassie blue staining method determined the concentration of TP while using an assay kit (#A405-2-2, Nanjing Jiancheng Bioengineering Institute, Nanjing, China).

2.3.8. The Effect on Phycobiliprotein

The extraction method of phycobiliprotein from *M. aeruginosa* is referred to as the method of Padgett et al. [39]. Firstly, 8 mL of the sample was centrifuged at $3000\times g$ and $4\text{ }^{\circ}\text{C}$ for 15 min. and the supernatant was discarded. Subsequently, the algal cells were washed and resuspended in 4 mL of PBS followed by being frozen and rapidly thawed three times. After centrifugation, the absorbance of the supernatant was finally measured at 565 nm, 620 nm, and 650 nm with a spectrophotometer.

The contents of PC, PE, APC, and PB were calculated, as follows:

$$\text{PC}(\text{mg/L}) = \frac{\text{OD}_{620} - 0.7 \times \text{OD}_{650}}{7.38} \quad (4)$$

$$\text{APC}(\text{mg/L}) = \frac{\text{OD}_{650} - 0.19 \times \text{OD}_{620}}{5.65} \quad (5)$$

$$\text{PE}(\text{mg/L}) = \frac{\text{OD}_{565} - 2.8 \times \text{PC} - 1.34 \times \text{APC}}{1.27} \quad (6)$$

$$\text{PB} = \text{PE} + \text{PC} + \text{APC} \quad (7)$$

3. Results and Discussion

3.1. Characterization of $\text{Cu}_2\text{O}/\text{SiO}_2$

3.1.1. X-ray Diffraction (XRD) & Scanning Electron Microscope (SEM)

Figure 1a shows the XRD patterns of Cu_2O , SiO_2 and $\text{Cu}_2\text{O}/\text{SiO}_2$. As can be seen from the Figure 1, there are five distinct diffraction peaks of pure Cu_2O ($2\theta = 29.5^{\circ}$, 36.3° , 42.3° , 61.3° , and 73.5°). The $\text{Cu}_2\text{O}/\text{SiO}_2$ synthesized by the solution phase method contains all of the characteristic peaks of Cu_2O , which indicates the successful synthesis of $\text{Cu}_2\text{O}/\text{SiO}_2$. Figure 1b shows the SEM image of $\text{Cu}_2\text{O}/\text{SiO}_2$. A large number of porous particles can be observed, because nano- SiO_2 covers the surface of Cu_2O . This is consistent with the morphology of the $\text{Cu}_2\text{O}-\text{SiO}_2$ nanoparticles observed by Xia et al. [40].

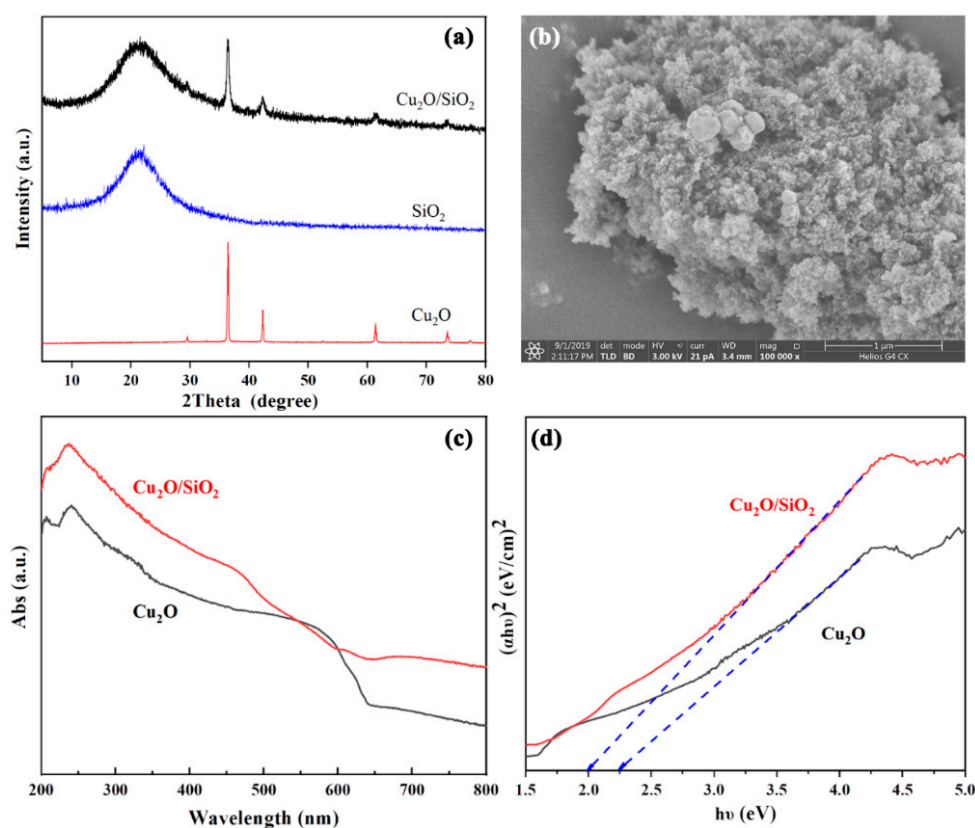


Figure 1. (a) X-ray diffraction (XRD) pattern of Cu₂O, SiO₂ and Cu₂O/SiO₂; (b) scanning electron microscope (SEM) image of Cu₂O/SiO₂; (c) UV-Vis patterns of Cu₂O and Cu₂O/SiO₂; and, (d) Tauc plot for pure Cu₂O and Cu₂O/SiO₂.

3.1.2. Ultraviolet-Visible Spectroscopy (UV-Vis)

Figure 1c provides the UV-Vis absorption spectra of the Cu₂O and Cu₂O/SiO₂. After coupling with SiO₂, the Cu₂O/SiO₂ exhibits strong absorption both in UV and visible light with a wavelength shorter than 480 nm, indicating the dramatically increased optical absorption of Cu₂O. The bandgap energy of pure Cu₂O and Cu₂O/SiO₂ were calculated through a Tauc plot of $(\alpha h\nu)^2$ vs. $h\nu$, as shown in Figure 1d. In accordance with formula (8), the band gap energy of Cu₂O and Cu₂O/SiO₂ were calculated to be 2.24 and 2.01 eV, respectively. The narrowed bandgap indicated the possibility of Cu₂O/SiO₂ to enhance photocatalytic activity.

$$\alpha h\nu = K(h\nu - E_g)^{1/2} \quad (8)$$

where, α is the absorption coefficient, K represents a constant, $h\nu$ stands for the discrete photo energy, and E_g is the band gap energy.

3.2. Growth Inhibition of Cu₂O/SiO₂ on Algal Cells

Figure 2 shows the growth situation of *M. aeruginosa* after treatment with different concentrations of Cu₂O/SiO₂ during the experiment for the first time. As shown in Figure 2c, algae exposed to 10, 20, and 50 mg/L Cu₂O/SiO₂ had varying degrees of fading during the experiment. It can be seen from Figure 2a that the OD₆₈₀ value of *M. aeruginosa* in the control group gradually increased during the experiment, indicating that the algae cells were in good condition. Low concentrations of Cu₂O/SiO₂ (0.1, 1, and 5 mg/L) may promote the growth of *M. aeruginosa*, presumably because low doses of Cu²⁺ will promote the growth of *M. aeruginosa*. Duong et al. [17] found that 0.001 mg/L nano-Ag could not inhibit the growth of *M. aeruginosa*. The OD₆₈₀ value of *M. aeruginosa* exposed to 10, 20, and 50 mg/L

$\text{Cu}_2\text{O}/\text{SiO}_2$ showed a downward trend, and 10 mg/L $\text{Cu}_2\text{O}/\text{SiO}_2$ had the strongest inhibitory effect on the growth of *M. aeruginosa*. The OD_{680} value of *M. aeruginosa* exposed to 20 and 50 mg/L $\text{Cu}_2\text{O}/\text{SiO}_2$ was higher than 10 mg/L $\text{Cu}_2\text{O}/\text{SiO}_2$ in the later stage of the experiment, which was probably due to the absorbance of high concentration nanomaterials. As shown in Figure 2b, the inhibition rate of $\text{Cu}_2\text{O}/\text{SiO}_2$ to *M. aeruginosa* gradually increased during the experiment, which could reach 297% at 120 h, indicating that $\text{Cu}_2\text{O}/\text{SiO}_2$ could inhibit the growth of the algae to some extent.

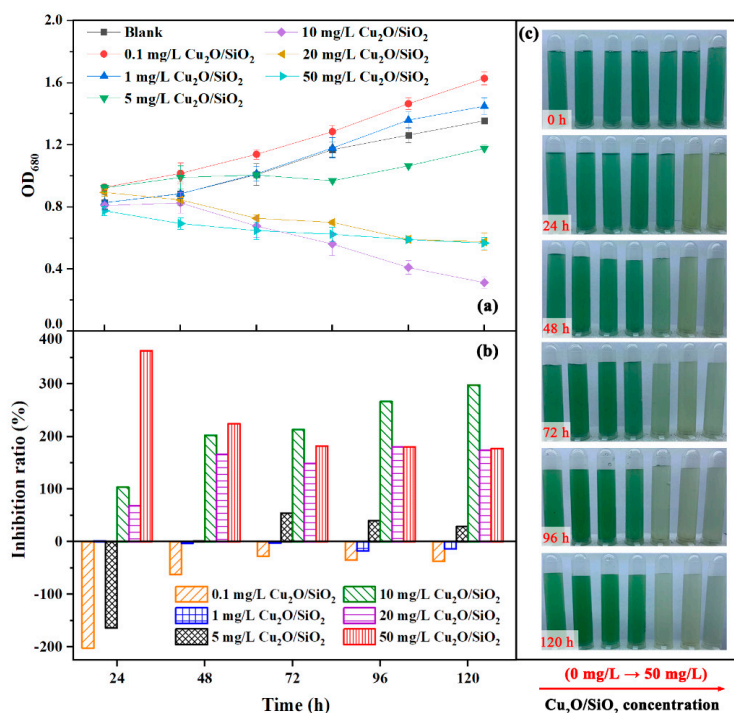


Figure 2. The growth of *M. aeruginosa* after treatment with different concentrations of $\text{Cu}_2\text{O}/\text{SiO}_2$. (a) OD_{680} value; (b) Inhibition rate; and, (c) The color change of algae during the experiment.

3.3. Mechanism of $\text{Cu}_2\text{O}/\text{SiO}_2$ Inhibiting Algae Growth

3.3.1. Metal Ions

The red line in Figure 3 shows the Cu^{2+} concentration released by 10 mg/L $\text{Cu}_2\text{O}/\text{SiO}_2$ in the solution. The amount of Cu^{2+} released by $\text{Cu}_2\text{O}/\text{SiO}_2$ increased at the beginning of the experiment and reached equilibrium at 24 h (about 0.55 mg/L). The OD_{680} values of *M. aeruginosa* that were exposed to $\text{Cu}_2\text{O}/\text{SiO}_2$ and $\text{CuSO}_4 \cdot 5\text{H}_2\text{O}$ (Cu^{2+}) are shown in the black line portion of Figure 3. The control group grew normally during the experiment, and the growth of *M. aeruginosa* exposed to 0.55 mg/L $\text{CuSO}_4 \cdot 5\text{H}_2\text{O}$ was immediately inhibited. The OD_{680} of *M. aeruginosa* exposed to 10 mg/L $\text{Cu}_2\text{O}/\text{SiO}_2$ initially increased and then rapidly decreased, eventually reaching 0.272. The inhibitory effect of 10 mg/L $\text{Cu}_2\text{O}/\text{SiO}_2$ on *M. aeruginosa* was higher than that of 0.55 mg/L $\text{Cu}_2\text{O}/\text{SiO}_2$, so the release of metal ions is considered to be a part of the mechanism of metal-containing nanomaterials inhibiting algae growth.

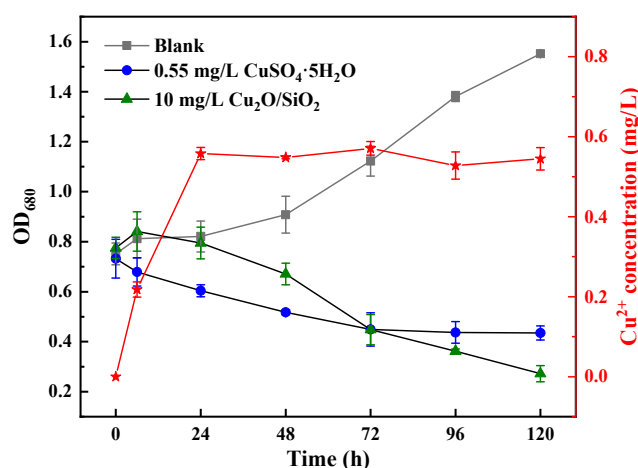


Figure 3. The concentration of Cu²⁺ released by Cu₂O/SiO₂ in solution and its effect on the growth of *M. aeruginosa*.

3.3.2. Chlorophyll *a*

Figure 4 shows the trend of the relative content of chlorophyll *a* during the experiment. The chlorophyll *a* content can also reflect the growth of *M. aeruginosa* from another side. By observing Figures 2a and 4, it can be found that the OD₆₈₀ value and the relative content chlorophyll *a* of *M. aeruginosa* have the same trend of variability during the experiment. The content of chlorophyll *a* of the *M. aeruginosa* in the control group grew continuously during the experiment, indicating that the algal cells in the control group grew well. The content of chlorophyll *a* in the algae cells that were exposed to 0.1 and 1 mg/L Cu₂O/SiO₂ increased with time and even exceeded the chlorophyll *a* content of the control group at 72–120 h, which indicates that low doses of Cu₂O/SiO₂ had no effect on the chlorophyll *a* of *M. aeruginosa*. The content of chlorophyll *a* in algae cells that were exposed to 10, 20, and 50 mg/L Cu₂O/SiO₂ decreased significantly and it was only about 25% of the initial content at 120 h. Similar results that were obtained by Hu et al. [41] showed that high doses of TiO₂ would inhibit the production of chlorophyll *a* in *Chrysophyta*. Based on the results above, it can be found that high doses of Cu₂O/SiO₂ (above 10 mg/L) would cause a decrease in the relative content chlorophyll *a* of *M. aeruginosa* and affect the growth of algae cells.

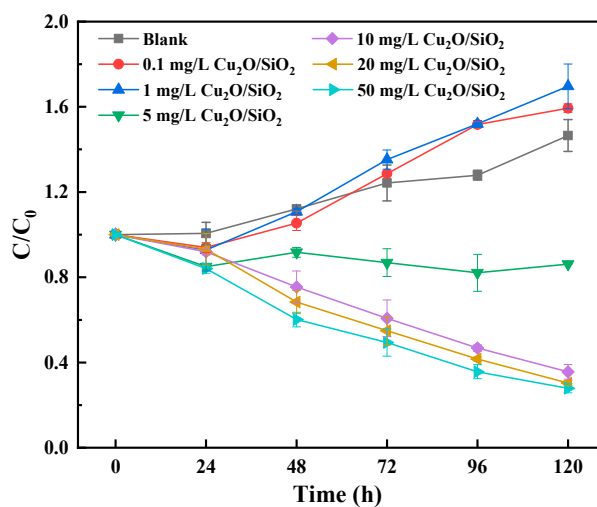


Figure 4. Effects of different concentrations of Cu₂O/SiO₂ on the content of chlorophyll *a* in *M. aeruginosa*.

3.3.3. ·OH Assays

Figure 5 shows the fluorescence spectrum of the $\text{Cu}_2\text{O}/\text{SiO}_2$ suspension. It can be found from Figure 5 that the experimental group showed an obvious fluorescence peak at 315 nm at 2 h and 6 h. The intensity of this fluorescent peak became stronger over time, indicating that continuous illumination will promote the production of ·OH by $\text{Cu}_2\text{O}/\text{SiO}_2$. The intensity of the fluorescent peak of the control group was significantly lower than that of the experimental group, because ·OH was continuously quenched by isopropanol. From this experiment, it can be found that, when being added in the solution, $\text{Cu}_2\text{O}/\text{SiO}_2$ would produce a small amount of ·OH immediately, and the amount of ·OH would increase with the increase of illumination time.

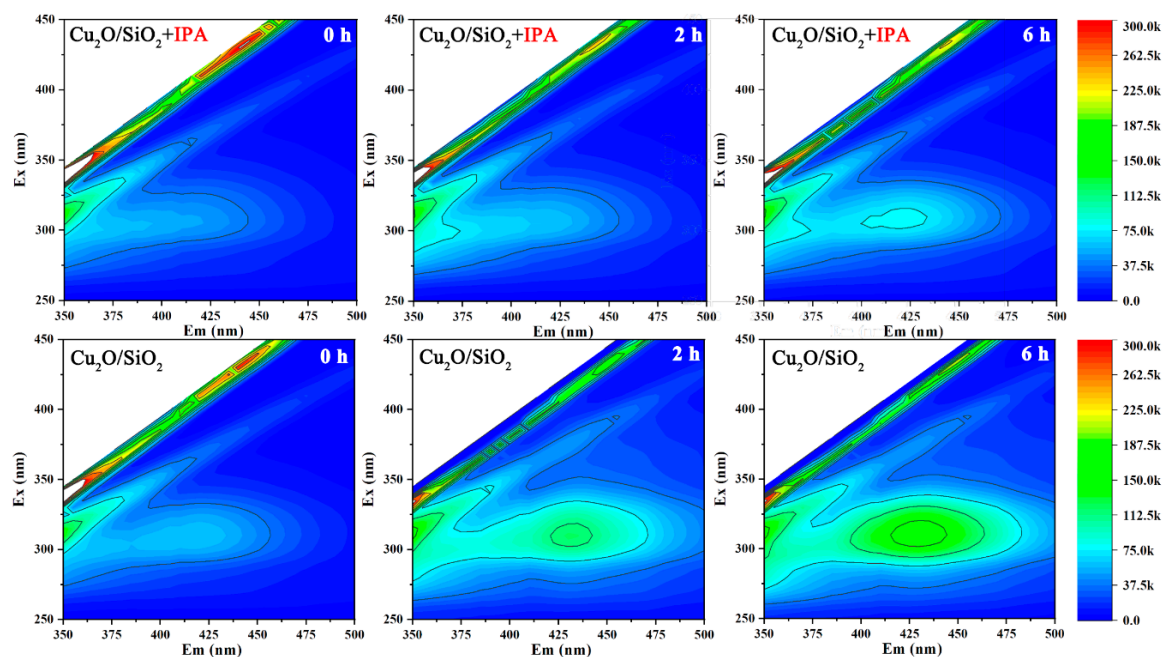


Figure 5. Excitation-emission matrix (EEM) diagram of ·OH concentration change with time.

3.3.4. Active Species Trapping Experiments

Figure 6 shows the trends of the three kinds of ROS during the active species trapping experiments. As shown in Figure 6, IPA and SO have a slight effect on the growth of algae cells, while BQ could inhibit the growth of algae cells. The relative inhibition rate of $\text{Cu}_2\text{O}/\text{SiO}_2$ to *M. aeruginosa* decreased from 189% to 162% after the addition of IPA. However, the inhibitory effect of $\text{Cu}_2\text{O}/\text{SiO}_2$ on the growth of *M. aeruginosa* after adding BQ and SO was not significantly different from that of pure $\text{Cu}_2\text{O}/\text{SiO}_2$. Therefore, it can be inferred that ·OH is the main active substance in the experiment based on the experimental results.

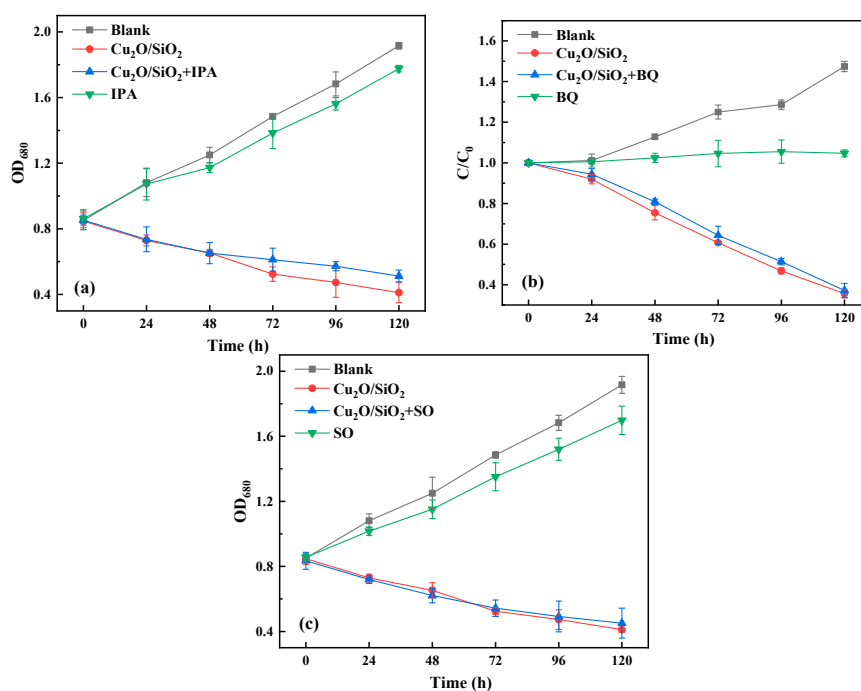


Figure 6. Active species trapping experiments. (a) $\cdot\text{OH}$; (b) $\cdot\text{O}_2^-$; and, (c) h^+ .

3.3.5. Antioxidant Enzyme

Figure 7 shows the effect of Cu₂O/SiO₂ on the activities of antioxidant enzymes of *M. aeruginosa*. The SOD activity of the control group algae floated within a certain range, while the SOD activity of the experimental group sharply decreased at the beginning of the experiment and remained relatively stable thereafter. It indicates that, when exposed to Cu₂O/SiO₂, the SOD of *M. aeruginosa* began to scavenge free radicals to inhibit oxidative damage. This is consistent with the study by Hazani et al. [42]. They found a significant decrease in the SOD activity of *Chlorella* and *Dunaliella salina* that were exposed to 100 and 200 mg/L of nano-Ag. The change in CAT activity of algal cells during the experiment is shown in Figure 7b. It can be found that the CAT activity of *M. aeruginosa* rapidly rose and then remained at a higher level as the experiment progressed. It is speculated that, in the early stage of the experiment, Cu₂O/SiO₂ will cause an increase in H₂O₂ content within algae cells, thus promoting CAT activity to protect against oxidative stress.

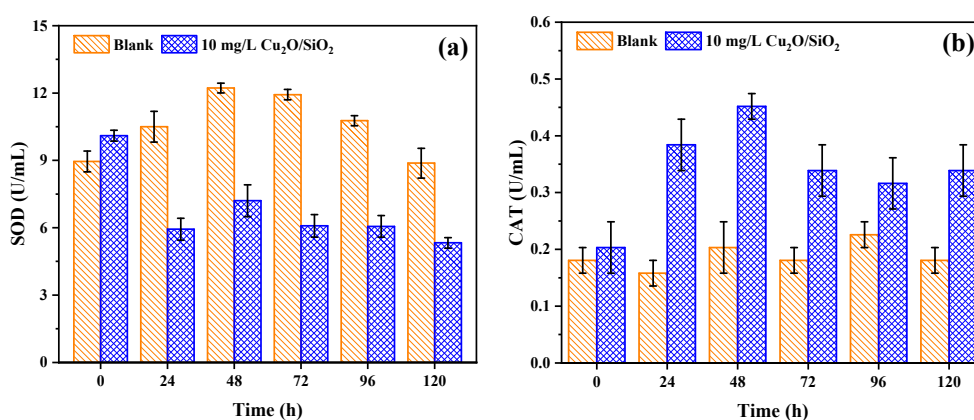


Figure 7. Changes of (a) superoxide dismutase (SOD) and (b) catalase (CAT) activities during algae removal by Cu₂O/SiO₂.

3.3.6. EOM & IOM

Figure 8 presents the fluorescence spectra of EOM and IOM of algae cells. It was observed that the fluorescence spectrum of the IOM & EOM of algae contained peak A, $\lambda_{ex}/\lambda_{em} = 275/320$ nm; peak B, $\lambda_{ex}/\lambda_{em} = 225/325$ nm; peak C, $\lambda_{ex}/\lambda_{em} = 275/450$ nm; and, peak D, $\lambda_{ex}/\lambda_{em} = 450/350$ nm.

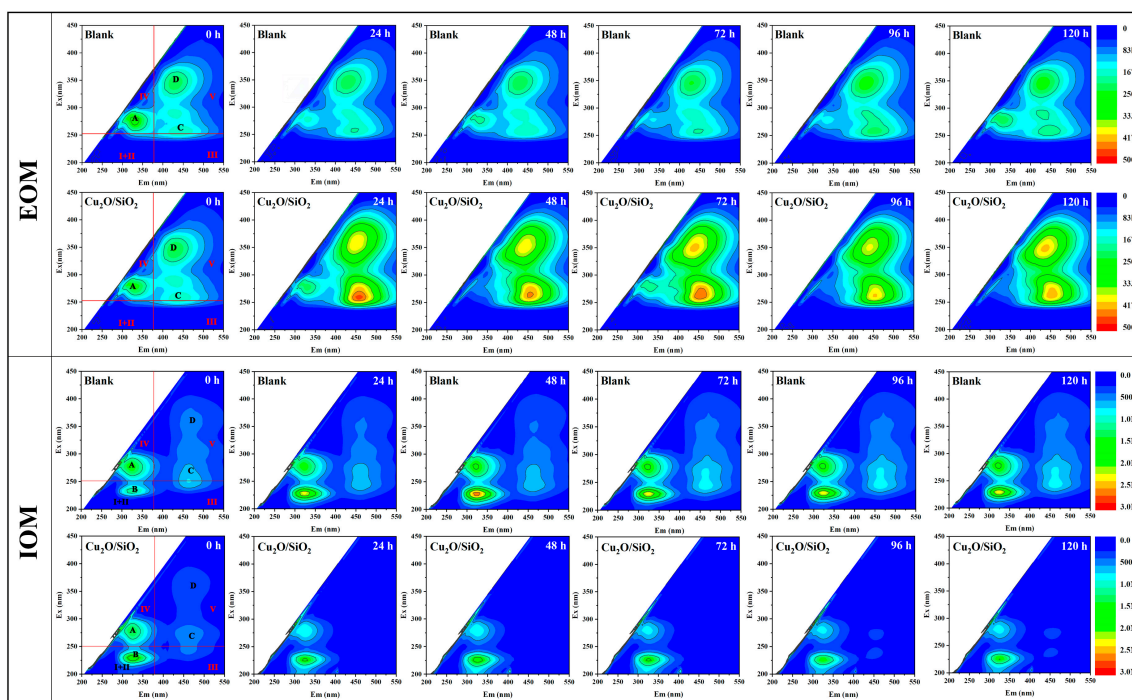


Figure 8. The fluorescence spectrum of extracellular organic matter (EOM) & intracellular organic matter (IOM) of algae cells.

A reduction in the intensities of peaks A, C, and D (represent aromatic proteins, fulvic acid substance, and humic acid substance, respectively) observed in the experimental group in Figure 8 indicates that the IOM of the algal cells was changed by $\text{Cu}_2\text{O}/\text{SiO}_2$. The fluorescence intensity of the peak A (protein-like substance) of the EOM of the experimental group algae cells gradually weakened, and the fluorescence intensity of the peak C (fulvic acid substance) and the peak D (humic acid substance) increased. This indicates that *M. aeruginosa* released a large amount of fulvic acid substance and humic acid substance after exposure to $\text{Cu}_2\text{O}/\text{SiO}_2$, and the proteinoid substance in the algae liquid was converted into fulvic acid substance and humic acid substance.

3.3.7. Total Protein

Figure 9 shows the total protein content of *M. aeruginosa* during the experiment. The total protein content of the control group algae increased continuously during the experiment, which was consistent with the trend of OD_{680} and chlorophyll *a* in Sections 2.2.2 and 3.2. The total protein of the algae cells in the experimental group continued to decrease during the experiment and finally stabilized at 0.00497 mg/mL, which was 5.7% of the initial total protein content. It is speculated that the membrane protein of *M. aeruginosa* was damaged, and the ROS entering the cell destroyed the protein synthesis chain, resulting in a decrease in protein content.

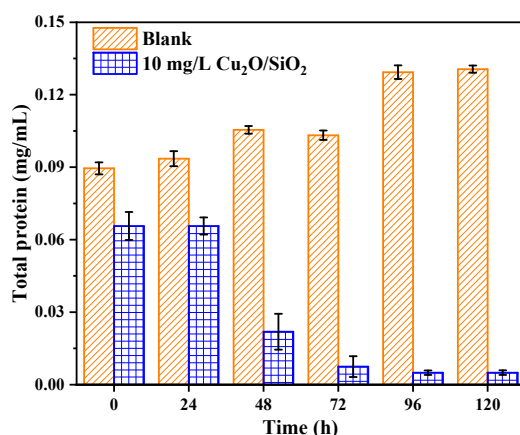


Figure 9. Changes in total protein content of algae during the experiment.

3.3.8. Phycobiliprotein

Figure 10 shows the changes in PB and PBP during the experiment. It can be seen from Figure 10 that the PC content of *M. aeruginosa* exposed to 10 mg/L showed a downward trend during the experiment, which was 10.5% of the control group at 120 h. A similar trend was observed in the changes of APC, PE, and PB in the algae cells of the experimental group, which were 39.7%, 46.1%, and 38.7% of the control group at 120 h, respectively. Similarly, it is speculated that the ROS produced by Cu₂O/SiO₂ might enter the interior of the cell, thereby destroying the phycobiliprotein, thus affecting the photo-harvesting ability of algal cells. This might be one of the mechanisms by which Cu₂O/SiO₂ inhibits the growth of *M. aeruginosa*.

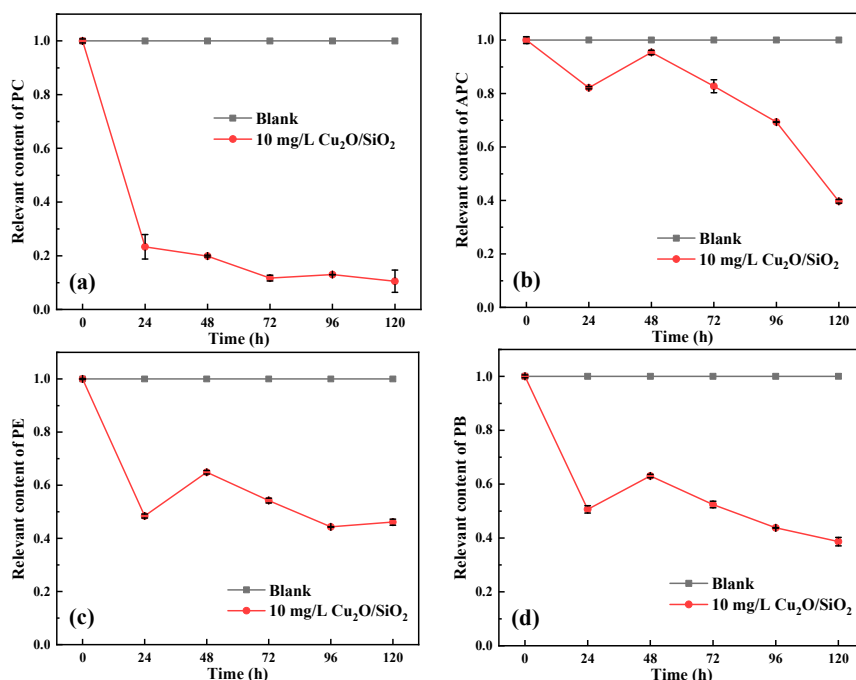


Figure 10. Changes of (a) phycocyanin, (b) allophycocyanin, (c) phycoerythrin, and (d) phycobiliprotein content of algae during the experiment.

3.3.9. Mechanism of Cu₂O/SiO₂ Inhibit the Growth of Algal Cells

In summary, Figure 11 systematically summarizes the mechanism by which Cu₂O/SiO₂ inhibits the growth of *M. aeruginosa*. First, Cu₂O/SiO₂ will release ·OH under the irradiation of visible light,

affecting the activity of SOD and CAT in algae cells, and causing oxidative damage. Second, $\text{Cu}_2\text{O}/\text{SiO}_2$ will damage chlorophyll *a* and phycobiliprotein, which affects the photo-harvesting ability of algae cells. The damage of the photosynthetic system will affect algae cells' ability to synthesize proteins, resulting in a decrease in total protein content and changes in IOM, and finally cause the death of algae cells. Moreover, $\text{Cu}_2\text{O}/\text{SiO}_2$ will release Cu^{2+} in solution and produce ionic toxicity to *M. aeruginosa*.

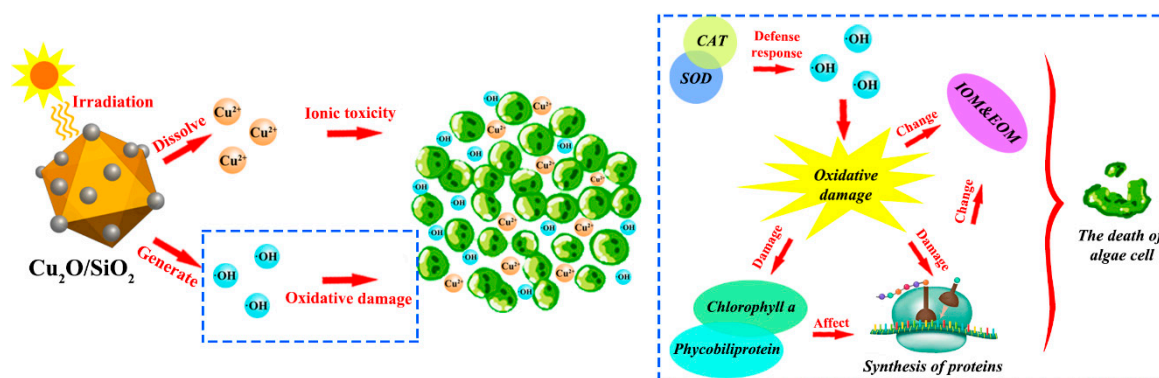


Figure 11. Mechanism of $\text{Cu}_2\text{O}/\text{SiO}_2$ inhibiting algae growth.

4. Conclusions

According to the analysis above, it can be concluded that the $\text{Cu}_2\text{O}/\text{SiO}_2$ possesses the characteristics of novel material, low cost, low doses, high inhibitory effects, and good visible light responding. Low doses of $\text{Cu}_2\text{O}/\text{SiO}_2$ (10 mg/L) will inhibit the growth of *M. aeruginosa* under low-intensity visible light. In terms of the inhibition mechanism of algae by $\text{Cu}_2\text{O}/\text{SiO}_2$, the Cu^{2+} released from $\text{Cu}_2\text{O}/\text{SiO}_2$ can cause metal toxicity to *M. aeruginosa*. At the same time, $\text{Cu}_2\text{O}/\text{SiO}_2$ will release $\cdot\text{OH}$ in the solution, which will reduce the activity of SOD and increase the activity of CAT, eventually leading to oxidative damage. Besides, $\text{Cu}_2\text{O}/\text{SiO}_2$ will affect the physiological characteristics of algae cells, which causes a decrease in the content of chlorophyll *a*, total protein, and phycobiliprotein, which results in damage, even the death of algae cells. In summary, this study will provide a new direction for the use of $\text{Cu}_2\text{O}/\text{SiO}_2$ to treat harmful cyanobacteria blooms.

Author Contributions: G.F. and B.W. conceptualized and supervised. M.B. and J.L. performed experimental work. All the authors contributed in writing, editing, and analysis.

Funding: This research was funded by the Technical Research Project of Shenzhen Municipal Science and Technology Innovation Commission in China (NO. 20170422), the National Natural Science Foundation of China (No. 51778146), the Outstanding Youth Fund of Fujian Province in China (No. 2018J06013) and the Open Project Program of National Engineering Research Center for Environmental Photocatalysis (No. NERCEP-201901).

Acknowledgments: The authors would like to thank the reviewers and editors for their valuable remarks and comments that greatly improved the quality of the paper.

Conflicts of Interest: There are no conflict to declare.

References

1. Paerl, H.W.; Paul, V.J. Climate change: Links to global expansion of harmful cyanobacteria. *Water Res.* **2012**, *46*, 1349–1363. [CrossRef] [PubMed]
2. Yan, Q.Y.; Yu, Y.H.; Feng, W.S.; Pan, G.; Chen, H.; Chen, J.; Yang, B.; Li, X.M.; Zhang, X. Plankton Community Succession in Artificial Systems Subjected to Cyanobacterial Blooms Removal using Chitosan-Modified Soils. *Microb. Ecol.* **2009**, *58*, 47–55. [CrossRef] [PubMed]
3. Bakheet, B.; Islam, M.A.; Beardall, J.; Zhang, X.W.; McCarthy, D. Effective electrochemical inactivation of *Microcystis aeruginosa* and degradation of microcystins via a novel solid polymer electrolyte sandwich. *Chem. Eng. J.* **2018**, *350*, 616–626. [CrossRef]

4. Starling, F.L.D.R. Control of eutrophication by silver carp (*Hypophthalmichthys molitrix*) in the tropical Paranoá Reservoir (Brasília, Brazil): A mesocosm experiment. *Hydrobiologia* **1993**, *257*, 143–152. [[CrossRef](#)]
5. Kondzior, P.; Butarewicz, A. Effect of Heavy Metals (Cu and Zn) on the Content of Photosynthetic Pigments in the Cells of Algae *Chlorella vulgaris*. *J. Ecol. Eng.* **2018**, *19*, 18–28. [[CrossRef](#)]
6. Park, J.; Church, J.; Son, Y.; Kim, K.T.; Lee, W.H. Recent advances in ultrasonic treatment: Challenges and field applications for controlling harmful algal blooms (HABs). *Ultrason. Sonochem.* **2017**, *38*, 326–334. [[CrossRef](#)]
7. Wang, J.X.; Zhang, X.Z.; Chen, Y.S.; Sommerfeld, M.; Hu, Q. Toxicity assessment of manufactured nanomaterials using the unicellular green alga *Chlamydomonas reinhardtii*. *Chemosphere* **2008**, *73*, 1121–1128. [[CrossRef](#)]
8. Zhao, J.; Cao, X.; Wang, Z.; Dai, Y.; Xing, B. Mechanistic understanding toward the toxicity of graphene-family materials to freshwater algae. *Water Res.* **2017**, *111*, 18–27. [[CrossRef](#)]
9. Gu, N.; Gao, J.; Wang, K.; Li, B.; Dong, W.; Ma, Y. *Microcystis aeruginosa* inhibition by Zn-Fe-LDHs as photocatalyst under visible light. *J. Taiwan Inst. Chem. Eng.* **2016**, *64*, 189–195. [[CrossRef](#)]
10. Guo, R.; Wang, H.; Suh, Y.S.; Ki, J.S. Transcriptomic profiles reveal the genome-wide responses of the harmful dinoflagellate *Cochlodinium polykrikoides* when exposed to the algicide copper sulfate. *BMC Genom.* **2016**, *17*, 29. [[CrossRef](#)]
11. Abidi, M.; Assadi, A.A.; Bouzaza, A.; Hajjaji, A.; Bessais, B.; Rtimi, S. Photocatalytic indoor/outdoor air treatment and bacterial inactivation on Cu_xO/TiO₂ prepared by HiPIMS on polyester cloth under low intensity visible light. *Appl. Catal. B-Environ.* **2019**, *259*, 118074. [[CrossRef](#)]
12. Baghriche, O.; Rtimi, S.; Pulgarin, C.; Kiwi, J. Polystyrene CuO/Cu₂O uniform films inducing MB-degradation under sunlight. *Catal. Today* **2017**, *284*, 77–83. [[CrossRef](#)]
13. Guo, S.; Fang, Y.; Dong, S.; Wang, E. Templateless, surfactantless, electrochemical route to a cuprous oxide microcrystal: From octahedra to monodisperse colloid spheres. *Inorg. Chem.* **2007**, *46*, 9537–9539. [[CrossRef](#)] [[PubMed](#)]
14. Singh, D.P.; Neti, N.R.; Sinha, A.S.K.; Srivastava, O.N. Growth of different nanostructures of Cu₂O (nanowires, nanowires, and nanocubes) by simple electrolysis based oxidation of copper. *J. Phys. Chem. C* **2007**, *111*, 1638–1645. [[CrossRef](#)]
15. Cao, C.H.; Xiao, L.; Chen, C.H.; Cao, Q.H. Synthesis of novel Cu₂O/BiOCl heterojunction nanocomposites and their enhanced photocatalytic activity under visible light. *Appl. Surf. Sci.* **2015**, *357*, 1171–1179. [[CrossRef](#)]
16. Garcia, R.; Tello, M.; Moulin, J.F.; Biscarini, F. Size and shape controlled growth of molecular nanostructures on silicon oxide templates. *Nano Lett.* **2004**, *4*, 1115–1119. [[CrossRef](#)]
17. Duong, T.T.; Le, T.S.; Tran, T.T.H.; Nguyen, T.K.; Ho, C.T.; Dao, T.H.; Le, T.P.Q.; Nguyen, H.C.; Dang, D.K.; Le, T.T.H.; et al. Inhibition effect of engineered silver nanoparticles to bloom forming cyanobacteria. *Adv. Nat. Sci. Nanosci.* **2016**, *7*, 035018. [[CrossRef](#)]
18. Franklin, N.M.; Rogers, N.J.; Apte, S.C.; Batley, G.E.; Gadd, G.E.; Casey, P.S. Comparative toxicity of nanoparticulate ZnO, bulk ZnO, and ZnCl₂ to a freshwater microalga (*Pseudokirchneriella subcapitata*): The importance of particle solubility. *Environ. Sci. Technol.* **2007**, *41*, 8484–8490. [[CrossRef](#)]
19. Pakrashi, S.; Dalai, S.; Prathna, T.C.; Trivedi, S.; Myneni, R.; Raichur, A.M.; Chandrasekaran, N.; Mukherjee, A. Cytotoxicity of aluminium oxide nanoparticles towards fresh water algal isolate at low exposure concentrations. *Aquat. Toxicol.* **2013**, *132–133*, 34–45. [[CrossRef](#)]
20. Fan, G.D.; Bao, M.C.; Zheng, X.M.; Hong, L.; Zhan, J.J.; Chen, Z.; Qu, F.S. Growth inhibition of harmful cyanobacteria by nanocrystalline Cu-MOF-74: Efficiency and its mechanisms. *J. Hazard Mater.* **2019**, *367*, 529–538. [[CrossRef](#)]
21. Loprasert, S.; Vattanaviboon, P.; Praituan, W.; Chamngopol, S.; Mongkolsuk, S. Regulation of the oxidative stress protective enzymes, catalase and superoxide dismutase in *Xanthomonas*—A review. *Gene* **1996**, *179*, 33–37. [[CrossRef](#)]
22. Strzelczyk, J.K.; Wiczowski, A. Oxidative damage and carcinogenesis. *Contemp. Oncol. Pozn* **2012**, *16*, 230–233. [[CrossRef](#)] [[PubMed](#)]
23. Ling, F.; Hamzeh, M.; Dodard, S.; Zhao, Y.H.; Sunahara, G.I. Effects of TiO₂ nanoparticles on ROS production and growth inhibition using freshwater green algae pre-exposed to UV irradiation. *Environ. Toxicol. Pharmacol.* **2015**, *39*, 1074–1080.

24. Liu, W.; Au, D.W.T.; Anderson, D.M.; Lam, P.K.S.; Wu, R.S.S. Effects of nutrients, salinity, pH and light: Dark cycle on the production of reactive oxygen species in the alga *Chattonella marina*. *J. Exp. Mar. Biol. Ecol.* **2007**, *346*, 76–86. [[CrossRef](#)]
25. Zhou, H.; Wang, X.J.; Zhou, Y.; Yao, H.Z.; Ahmad, F. Evaluation of the toxicity of ZnO nanoparticles to *Chlorella vulgaris* by use of the chiral perturbation approach. *Anal. Bioanal. Chem.* **2014**, *406*, 3689–3695. [[CrossRef](#)]
26. Ali, E.M.; Khairy, H.M. Environmental assessment of drainage water impacts on water quality and eutrophication level of Lake Idku, Egypt. *Environ. Pollut.* **2016**, *216*, 437–449. [[CrossRef](#)]
27. Fang, X.; Mark, G.; Sonntag, C.V. OH radical formation by ultrasound in aqueous solutions Part I: The chemistry underlying the terephthalate dosimeter. *Ultrason. Sonochem.* **1996**, *3*, 57–63. [[CrossRef](#)]
28. Rad, M.; Dehghanpour, S. ZnO as an efficient nucleating agent and morphology template for rapid, facile and scalable synthesis of MOF-46 and ZnO@MOF-46 with selective sensing properties and enhanced photocatalytic ability. *RSC Adv.* **2016**, *6*, 61784–61793. [[CrossRef](#)]
29. Wang, X.; Wang, X.J.; Zhao, J.F.; Song, J.K.; Wang, J.Y.; Ma, R.R.; Ma, J.X. Solar light-driven photocatalytic destruction of cyanobacteria by F-Ce-TiO₂/expanded perlite floating composites. *Chem. Eng. J.* **2017**, *320*, 253–263. [[CrossRef](#)]
30. Oukarroum, A.; Zaidi, W.; Samadani, M.; Dewez, D. Toxicity of Nickel Oxide Nanoparticles on a Freshwater Green Algal Strain of *Chlorella vulgaris*. *BioMed. Res. Int.* **2017**, *2017*, 1–8. [[CrossRef](#)]
31. Ma, S.; Zhan, S.; Jia, Y.; Zhou, Q. Superior Antibacterial Activity of Fe₃O₄-TiO₂ Nanosheets under Solar Light. *ACS Appl. Mater. Interfaces* **2015**, *7*, 21875–21883. [[CrossRef](#)] [[PubMed](#)]
32. Manirafasha, E.; Murwanashyaka, T.; Ndikubwimana, T.; Yue, Q.; Zeng, X.H.; Lu, Y.H.; Jing, K.J. Ammonium chloride: A novel effective and inexpensive salt solution for phycocyanin extraction from *Arthrospira (Spirulina) platensis*. *J. Appl. Phycol.* **2017**, *29*, 1261–1270. [[CrossRef](#)]
33. Na, G.; Gao, J.; Li, H.; Wu, Y.; Ma, Y.; Wang, K. Montmorillonite-supported with Cu₂O nanoparticles for damage and removal of *Microcystis aeruginosa* under visible light. *Appl. Clay Sci.* **2016**, *132–133*, 79–89.
34. Zhicong, W.; Dunhai, L.; Hongjie, Q.; Yinxia, L. An integrated method for removal of harmful cyanobacterial blooms in eutrophic lakes. *Environ. Pollut.* **2012**, *160*, 34–41.
35. Fan, G.D.; You, Y.F.; Wang, B.; Wu, S.M.; Zhang, Z.; Zheng, X.M.; Bao, M.C.; Zhan, J.J. Inactivation of harmful cyanobacteria by Ag/AgCl@ZIF-8 coating under visible light: Efficiency and its mechanisms. *Appl. Catal. B Environ.* **2019**, *256*, 117866. [[CrossRef](#)]
36. Tian, C.; Guo, T.T.; Liu, R.P.; Jefferson, W.; Liu, H.J.; Jiu-Hui, Q.U. Formation of disinfection by-products by *Microcystis aeruginosa* intracellular organic matter: Comparison between chlorination and bromination. *Huan Jing Ke Xue* **2013**, *34*, 4282–4289.
37. Qu, F.; Liang, H.; Wang, Z.; Wang, H.; Yu, H.; Li, G. Ultrafiltration membrane fouling by extracellular organic matters (EOM) of *Microcystis aeruginosa* in stationary phase: Influences of interfacial characteristics of foulants and fouling mechanisms. *Water Res.* **2012**, *46*, 1490–1500. [[CrossRef](#)]
38. Tao, Y.; Mao, X.; Hu, J.; Mok, H.O.; Wang, L.; Au, D.W.; Zhu, J.; Zhang, X. Mechanisms of photosynthetic inactivation on growth suppression of *Microcystis aeruginosa* under UV-C stress. *Chemosphere* **2013**, *93*, 637–644. [[CrossRef](#)]
39. Padgett, M.P.; Krogmann, D.W. Large scale preparation of pure phycobiliproteins. *Photosynth. Res.* **1987**, *11*, 225–235. [[CrossRef](#)]
40. Yang, X.; Yuan, R.; Chai, Y.; Zhuo, Y.; Hong, C.; Liu, Z.; Su, H. Porous redox-active Cu₂O-SiO₂ nanostructured film: Preparation, characterization and application for a label-free amperometric ferritin immunosensor. *Talanta* **2009**, *78*, 596–601. [[CrossRef](#)]
41. Hu, J.; Wang, J.; Liu, S.; Zhang, Z.; Zhang, H.; Cai, X.; Pan, J.; Liu, J. Effect of TiO₂ nanoparticle aggregation on marine microalgae *Isochrysis galbana*. *J. Environ. Sci. China* **2018**, *66*, 208–215. [[CrossRef](#)] [[PubMed](#)]
42. Hazani, A.A.; Ibrahim, M.M.; Arif, I.A.; Shehata, A.I.; El-Gaaly, G.; Daoud, M.; Fouad, D.; Rizwana, H.; Moubayed, N. Ecotoxicity of Ag-Nanoparticles to Microalgae. *J. Pure Appl. Microbiol.* **2013**, *7*, 233–241.

